Development of a Digital Microscope for the Characterization of Defects in Cryogenic DT-filled

Targets

Joy Zhang

Penfield High School

Advisor: Roger Janezic

Laboratory for Laser Energetics

University of Rochester

Rochester, NY

September 2017

1. Abstract

A digital microscope is being developed for the purpose of viewing submicron defects on the surface of cryogenic deuterium-tritium (DT) filled targets. The existing target characterization system is aperture limited by a protective shroud, limiting its resolution to 1.6 μm. The microscope under development will eventually operate in a cryostat where targets can be viewed directly without the limitations of a protective shroud. This will allow the microscope to operate from a shorter working distance, improving its resolution to approximately 0.5 μm. A U.S. Air Force resolution target was used to generate pixel-profile lineouts in order to quantify image quality during the optimization of illumination conditions. Using objectives of various magnifications, the optimal magnifying power of the microscope was determined. Additionally, the illumination conditions, including the wavelength, current, and exposure time of the light-emitting-diode (LED) light source, were optimized at ambient conditions. Under optimized conditions, a resolution of 0.5 μm was confirmed using polymer microsphere standards and 0.5-μm-diameter defects on a polystyrene (CH) cryogenic shell.

2. Introduction

Direct-drive inertial confinement fusion harnesses the potential of nuclear fusion as an abundant source of clean, safe energy through imploding cryogenic targets filled with solid DT fuel.[1] This can be done by placing the cryogenic DT-filled target (at 18 K) in the center of the OMEGA target chamber, where 60 high-energy pulsed beams are fired, causing the CH shell of the target to ablate outward.[2] This causes the DT fuel to compress rapidly and forcefully, generating the extreme densities and temperatures needed to initiate fusion reactions. Figure 1 shows two images of a typical cryogenic DT target, taken by the current target viewing system,

the optical Characterization Station, with two different focal points. Image (a) focuses upon the edge of the target shell and the ice layer that has formed within it and Image (b) focuses upon a defect upon the surface of the target shell.

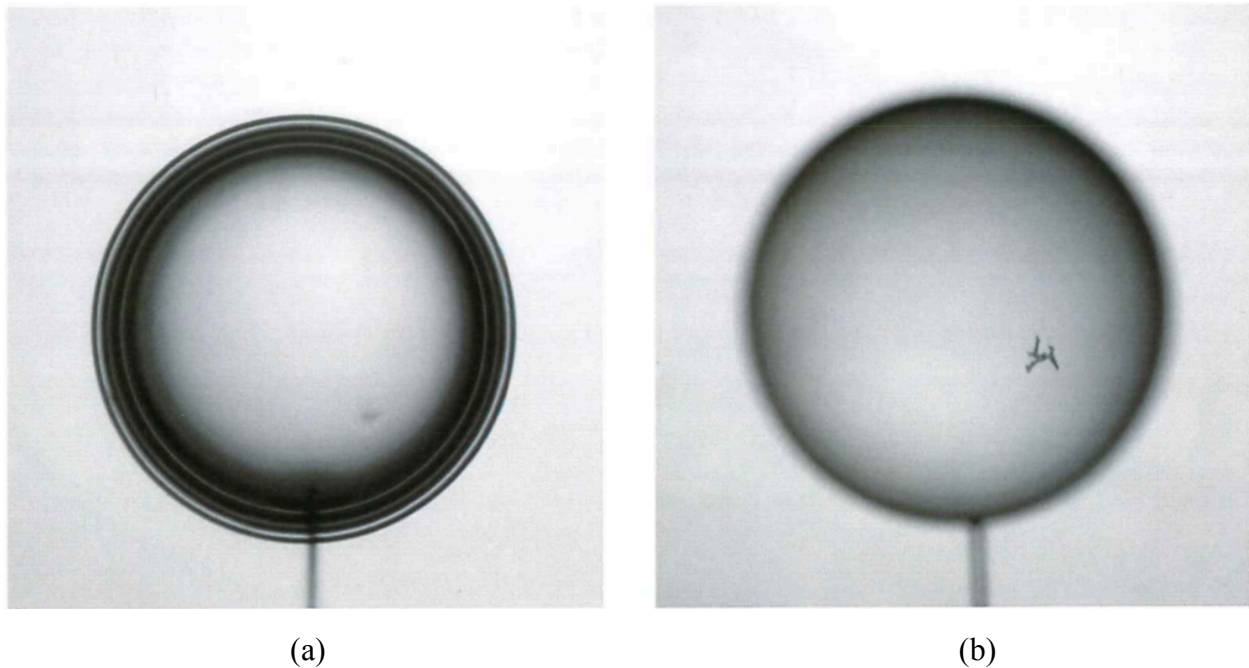<div align="center">(a)   (b)</div>

Figure 1: Images of a CH cryogenic shell taken by the Characterization Station. Image (a) focuses upon the shell's edge and image (b) focuses upon a dendrite defect on its surface (from Ref. 4).

In order to reach the desired densities and temperatures, the DT ice layer must be compressed uniformly, maintaining its spherical symmetry during the implosion. However, imperfections on the target's inner and outer surfaces may seed instabilities during implosion. In particular, the Rayleigh-Taylor instability causes non-uniformities in the interface between two materials of different densities to grow.[1] Therefore, in order to achieve desired core temperatures and densities, the target surface must contain minimal defects. However, there may be sub-micron defects on or within the shell surface that are currently not observed, consisting possibly

of metallic dust, condensable gases, or of some other material, that are hindering the desired densities and temperatures from being reached.[3] The Characterization Station does not possess a high enough resolving power to view these submicron defects. This is largely due to the existence of a protective shroud around the target, which maintains a cryogenic environment in order to allow the DT ice layer to form.[3] This protective shroud contains windows through which the Characterization Station views the target. However, these windows limit the cameras of the Characterization Station by requiring them to view the target from a distance, approximately 15 cm, which lowers their resolving power.[5] The measured resolution of the Characterization Station is approximately 3.1 μm, making it unable to resolve defects as small as 0.5 μm in diameter.[5]

3. Materials and Methods

In order to overcome the limitations of the protective shroud, a digital microscope apparatus was designed, which is intended to view the inner and outer surfaces of the target from within the Fill and Transfer Station #2 (FTS#2) cryostat.
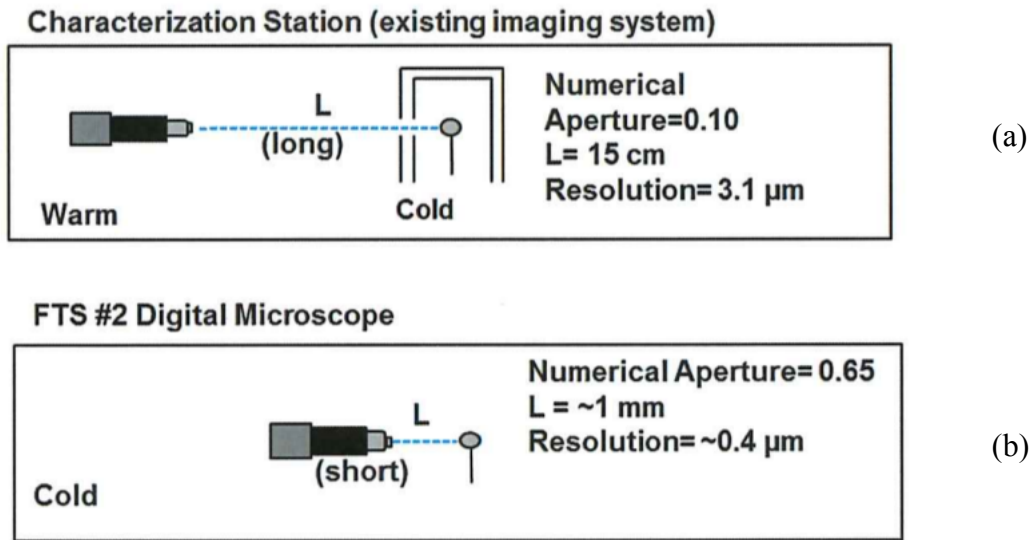
Characterization Station (existing imaging system)

L (long)

Warm   Cold

Numerical
Aperture=0.10
L= 15 cm
Resolution= 3.1 µm

(a)

FTS #2 Digital Microscope

L (short)

Cold

Numerical Aperture= 0.65
L = ~1 mm
Resolution= ~0.4 µm

(b)

Figure 2: Comparison between the Characterization Station (a) and FTS #2 Microscope (b).

The cryostat maintains a cryogenic environment in order to ensure the survival of the target's DT ice layer in its cryogenic state, during which target characterization is conducted.[3] Figure 2 shows that, by viewing the target from within the cryostat, the digital microscope would be able to image the target directly, from a distance of approximately 1 mm.[5] Additionally, the microscope objective of the digital microscope contains a larger numerical aperture (NA=0.65) compared to that of the Characterization Station (NA=0.10).[5] Numerical aperture is a measurement of a microscope objective's ability to capture light and resolve fine details at a fixed distance. Therefore, the larger numerical aperture of the digital microscope suggests that it would have higher resolving power, which is supported by the equation

$$R = \frac{\lambda}{2NA} \qquad (1)$$

where R is the resolution of the digital microscope, defined by the minimum distance between

two objects that is resolvable by an optical device, λ is the wavelength of the illumination source, and NA is the numerical aperture of the objective. It was projected that the apparatus designed for the FTS #2 digital microscope would provide a resolution of approximately 0.4 μm.
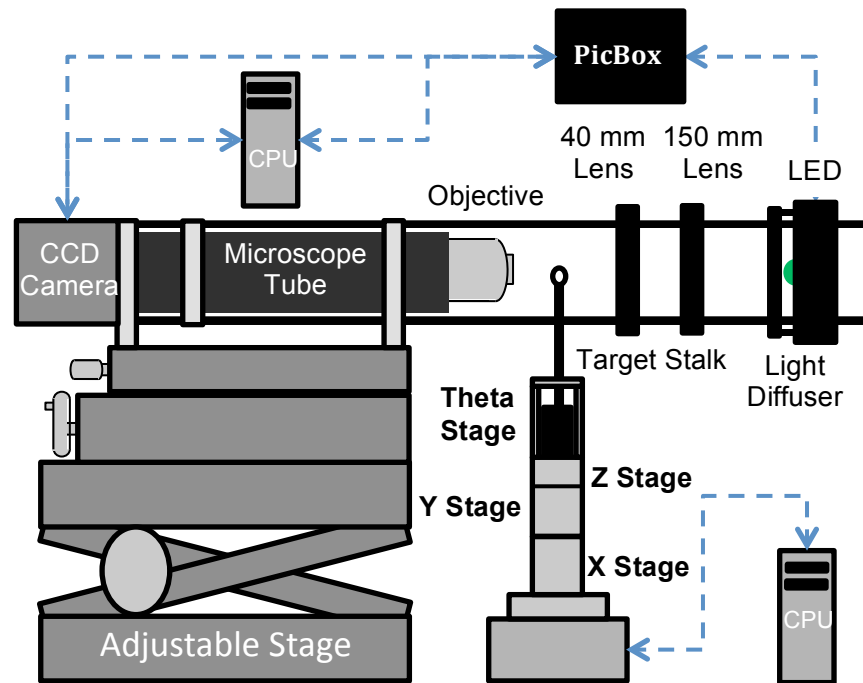

Figure 3: Box diagram of the microscope apparatus. The electronic communication pathways and the light path from the diffuser to the target are shown schematically.

The digital microscope shown in Figure 3 is composed of a microscope objective, a microscope tube, and a charge-coupled-device (CCD) camera. The digital microscope is mounted on an adjustable stage, which manipulates the objective's position. The target is illuminated by an LED, which emits light in rapid and continuous pulses. The LED's pulse rate is synchronized with the image capture rate of the camera by an LLE-designed "PicBox". This method utilizes the stroboscopic effect, in which the motion of an object is represented by a series of static snapshots that are repeatedly captured in synchronization with the pulses of light from the illumination source. The LED's rapid pulses stabilize the captured images of the target, mitigating the effects of the cryostat's vibration on the image. The PicBox and the CCD camera

are interfaced to a computer (CPU), which allows the camera to capture images and contains a

set of controls which manipulate the LED's illumination settings such as the exposure time, the
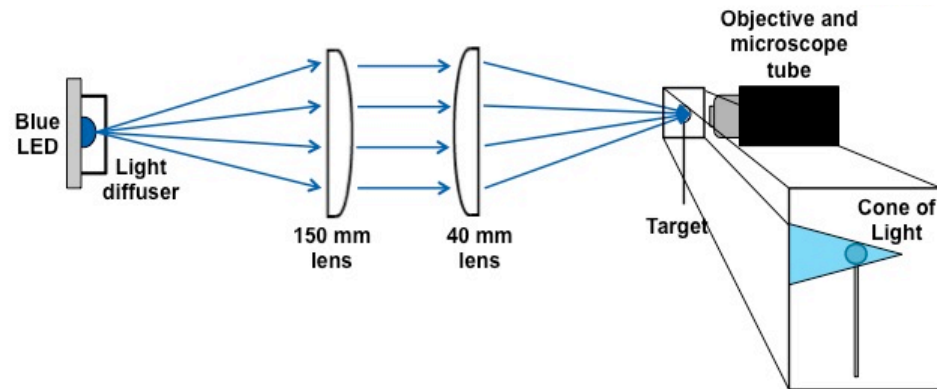
trigger rate, and the current.

Figure 4: Optical configuration for target illumination. The light pathway is shown schematically.

Figure 4 shows the pathway of light from the LED to the target. The light from the LED

is propagated by a holographic optical diffuser, which causes it to spread in order to provide

consistent illumination. The light then passes through two plano-convex lenses. The first, which

has an approximate working distance of 150 mm, collimates the light, making the rays accurately

parallel. The light then passes through the second lens, with an approximate working distance of

40 mm, which focuses the light onto the target in order to illuminate it. Optimally, the cone of

focused light illuminates the target tangentially as shown in the inset. This illumination system

allows the apparatus to utilize the methods of bright-field microscopy.

The apparatus also includes a motion stage upon which the target stalk is mounted. The

motion stage allows the target to be moved in the x-plane, y-plane, and z-plane, and also allows

it to rotate (theta). The motion stage is interfaced to a computer, which contains a set of controls

to move the target.

Figure 5 shows an image of an 8 μm wall x 860 μm diameter plastic CH "cryo" shell that

was taken by the digital microscope. The dark features upon the shell's surface are surface defects that were created during the target fabrication process. The defect that is encircled in red has a diameter of approximately 8 μm. This is the type of shell that would be filled to create cryogenic DT-filled targets.
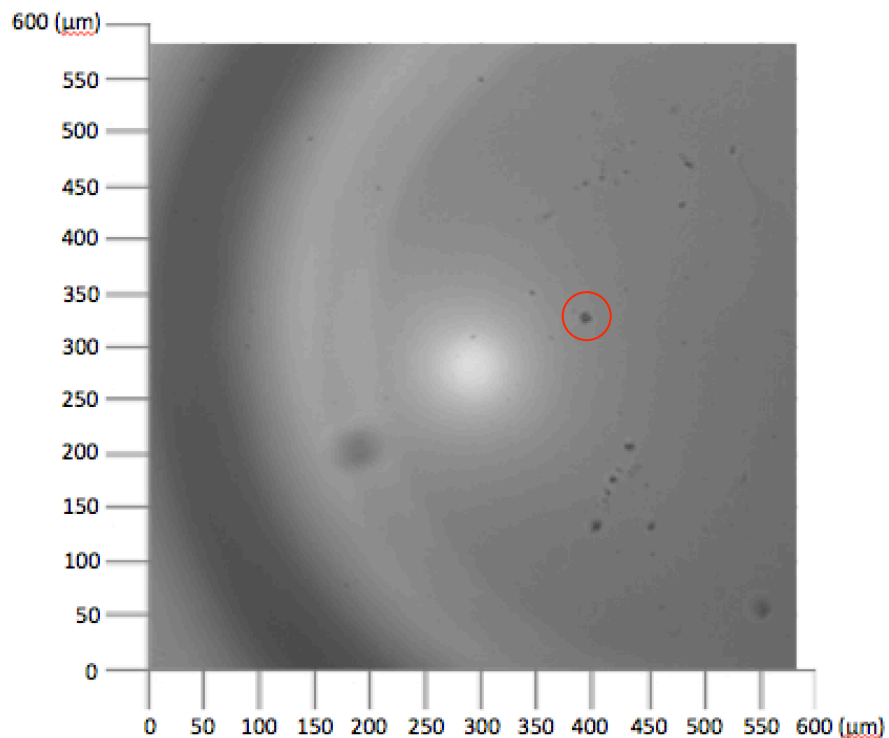

Figure 5. Typical image of a "cryo" shell employed for this study, captured with a 20x objective for the purpose of incorporating a larger view of the shell. The digital microscope's focus is upon defects on the shell's outer surface.

The digital microscope's working conditions were optimized in ambient conditions prior to its eventual placement in the FTS#2 cryostat. This ensured its ability to resolve 0.5-μm-diameter defects at room temperature before optimization occurs at cryogenic temperatures. A standard 1951 US Air Force resolution target, shown in Figure 6, was used for this optimization.
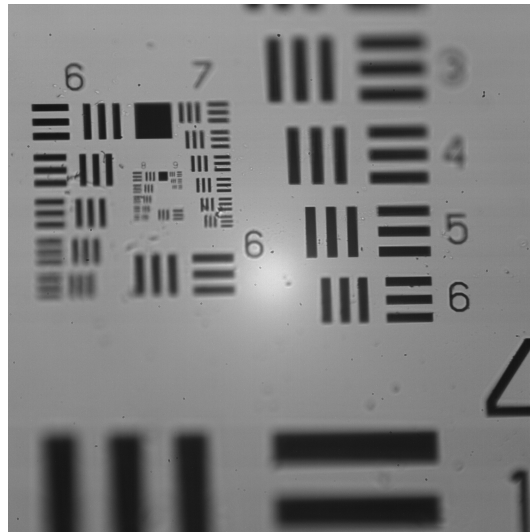
Figure 6. Image of an Air Force resolution target, captured with a 40x objective.

The resolution target is a plane of transparent glass that has a pattern of lines printed on it. These lines are organized into groups of three, which become progressively smaller towards the center of the target. The width of these lines decreases from 2000 μm to 0.55 μm. The resolution of the digital microscope was measured by determining the smallest distance between two lines that it was able to resolve.

Although the resolution target provided a fairly accurate estimation of the digital microscope's resolution, a more quantitative method to measure it was devised. Using an image of the resolution target that was taken by the digital microscope, a row of pixels that extended across a group of three lines was analyzed. The number of photons captured by each pixel was then graphed, generating a sine shaped curve, which is referred to as a pixel-profile lineout, shown in Figure 7. Then, the image's contrast ratio was calculated by dividing the highest number of photons collected by a single pixel by the lowest number of photons collected by a single pixel. Because contrast increases as resolving power increases, a higher contrast ratio

indicates a higher resolving power. For the image used to generate the pixel-profile lineout in Figure 7, the highest number of photons collected by a single pixel was 3270 and the lowest number of photons collected by a single pixel was 1038, yielding a contrast ratio of 3.2.
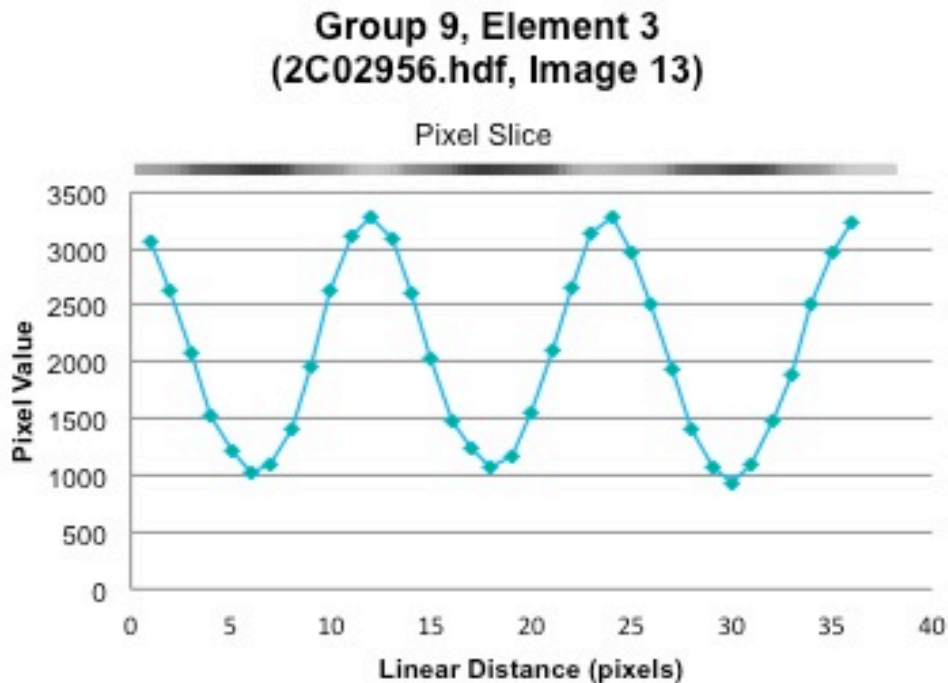

Figure 7. Pixel-profile lineout of a line group on the U.S. Air Force Resolution Target. 7.9 pixels correspond to 1 μm distance.

Another application of the resolution target is its use in creating a pixel-to-micron conversion scale. This was done by using software to determine how many pixels were present between two lines on the resolution target, whose separation is accurately known. For example, one pair of lines had a separation of 60 pixels and a separation width of 7.81 μm, which yielded a pixel-to-micron conversion of 7.67 pixels per μm.

Based on the average measurements of multiple line separations of different sizes for both the 20x and 40x objectives, it was determined that the conversion scale was approximately 4.2 pixels/μm for a 20x objective and 7.9 pixels/μm for a 40x objective. These measurements are

prone to slight error due to the resolving limitations of light microscopy, which may explain why the conversion scale for a 40x objective was not exactly twice as large as the conversion scale for a 20x objective, as would be expected. However, this conversion scale can be used to produce fairly accurate measurements of objects within the images captured by the digital microscope.

4. Optimization

In order to establish the optimal working conditions for the digital microscope, various factors were considered, including the wavelength of the LED and the illumination settings. Because a 40x objective provides twice as much magnification as a 20x objective, it provides the digital microscope with a higher resolving power. Figure 8 shows a comparison between two images of the resolution target, one taken with a 20x objective and one taken with a 40x objective. The smaller line groups on the resolution target are much more resolvable with the 40x objective than they are with the 20x objective.
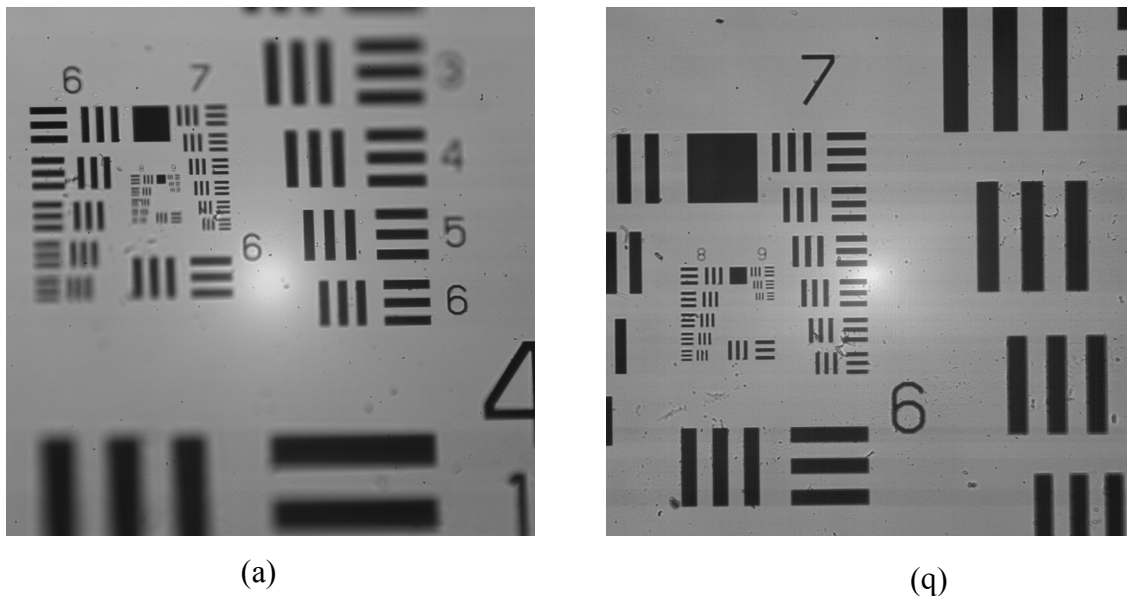

(a)   (q)

Figure 8. A comparison of images of the resolution target taken with a 20x objective (a) and a 40x objective (b).

It was calculated from Equation (1) that a 40x objective's numerical aperture of 0.65 would

yield a resolution of approximately 0.4 μm with green (525 nm) light illumination. This would make the goal of resolving 0.5 μm diameter defects feasible. Therefore, the 40x objective was utilized for most optimization operations.

4.1. LED Wavelength Optimization

Prior to the optimization of the LED's wavelength, a green (525 nm) LED was used as the digital microscope's illumination source. According to the spectral response of the CCD camera (E12 device), shown by the red curve in Figure 9, the camera's ability to collect photons is optimal when illuminated by light with wavelengths between 500 nm and 700 nm.
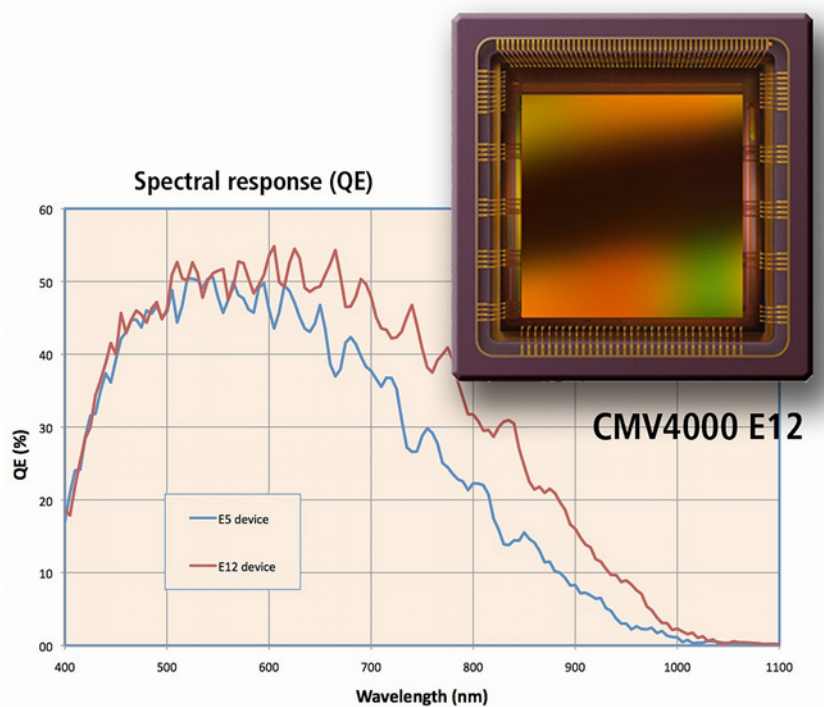

Figure 9. Spectral response graph for the complementary metal-oxide-semiconductor (CMOS) chip employed in the CCD camera (from Ref. 5). Quantum efficiency (QE) is shown as a function of wavelength of the illumination source. The chip design is shown in the top right corner.

However, according to Equation 1, as the wavelength of the LED decreases, the resolution value decreases as well, indicating a higher resolving power. Therefore, a blue LED, with a wavelength of 460 nm, was tested because it was predicted to yield a higher resolving power, although it is not considered optimal for the camera's spectral response.

Figure 10 shows the pixel-profile lineouts of resolution target images that were captured with the blue LED (right) and compared with lineouts of images taken with the green LED (left). Because the exposure time and current of the LED affect the resolution of the image, the images were taken over a range of exposure times and currents. The current for both LEDs ranged from 800 mA to 1400 mA while the exposure time ranged from 200 μs to 3000 μs. The contrast ratios at each setting were calculated for the pixel-profile lineouts. The highest contrast ratio for the blue LED was 4.0 at a setting of 1400 mA and 800 μs. The highest contrast ratio for the green LED was 3.7 at a setting of 1000 mA and 600 μs. Therefore, it was determined that the blue LED yielded a slightly higher resolving power. It should also be noted that the blue LED required a longer exposure time and higher current because of the camera's weaker spectral response due to the shorter wavelength.

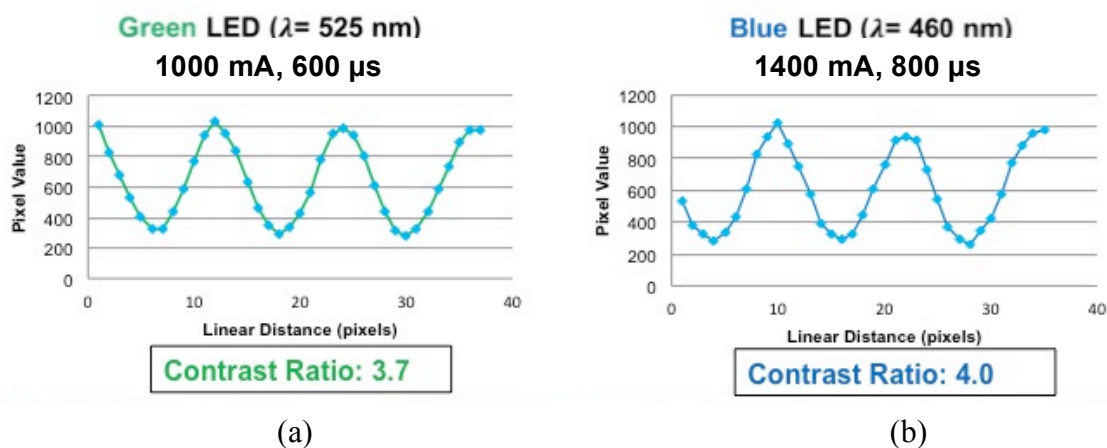(a)   (b)

Figure 10. Pixel-profile lineouts of resolution target images taken by the green LED (a) and the blue LED (b). The same group of three lines was used to generate both lineouts.

4.2 Current and Exposure Time Optimization

The computer interfaced to the CCD camera and PicBox utilizes the LLE "Cryoview" software to capture images and manipulate the LED settings. Cryoview allows the operator to easily manipulate the LED's current, exposure time (the length of each pulse from the LED), and trigger rate (the rate at which the LED pulses). The manipulation of these factors was expected to have an effect on the contrast ratio and image quality of the digital microscope. However, the trigger rate did not produce a profound effect on the image quality, and was therefore held constant at 5 Hz for the optimization process. During the optimization process, the current and exposure time were varied in order to determine which settings produced the highest image quality. The response of the contrast ratio to the variations of the LED's current and exposure time is shown in Figure 11. Because both factors have an effect on the image quality, the exposure time was kept constant at 800 μs while the current was varied. This exposure time was previously observed to produce moderate image quality. Current settings were tested within a range from 500 mA to 2,000 mA, beyond which the captured images exhibited poor image quality. Conversely, the current was kept constant at 1400 mA while the exposure time was varied. Exposure times were tested within a range from 200 μs to 3,000 μs, beyond which the captured images exhibited poor image quality.

Blue LED current optimization at 800 μs

(a)

○ Grainy: too little illumination

○ Best image quality
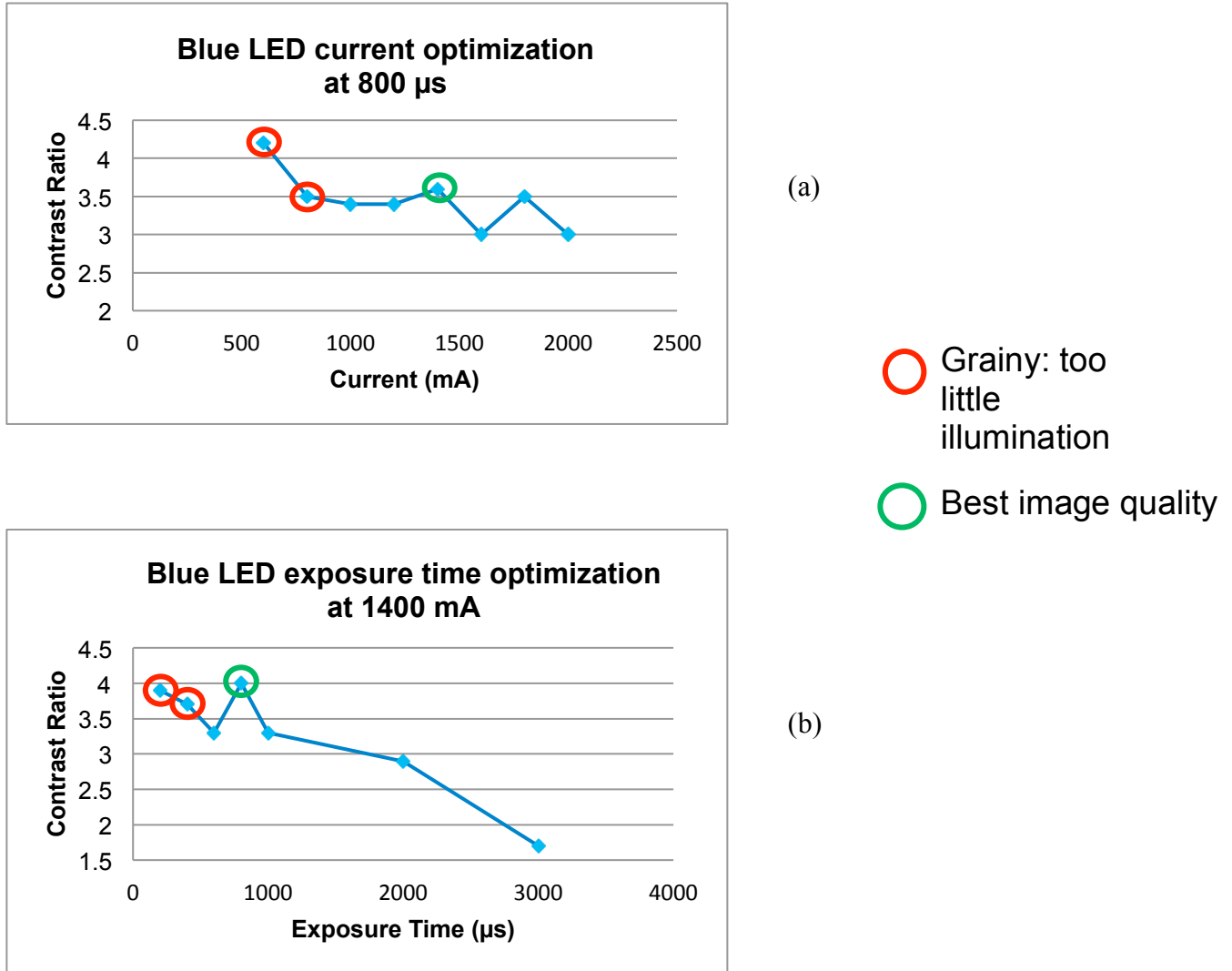
Blue LED exposure time optimization at 1400 mA

(b)

Figure 11. Contrast ratio as a function of LED current (a) and exposure time (b). The optimal current was found to be 1400 mA and the optimal exposure time was found to be 800 μs.

By capturing images of the resolution target under these illumination settings and generating pixel-profile lineouts in order to determine the contrast ratio, it was determined that the optimal current setting at an exposure time of 800 μs was 1400 mA while the optimal exposure time at a current of 1400 mA was 800 μs. Although during both optimization operations, illumination settings at the lower end of the tested ranges produced similar or higher contrast ratios, many of the images captured under these settings were grainy due to insufficient illumination.

5. Imaging of 0.5-μm microspheres and defects

After optimization operations were performed, 0.5-μm-diameter polymer microspheres[6] were imaged as an independent assessment of the resolving power of the microscope. These microspheres were prepared upon standard microscope slides. Images of these microspheres were captured, and it was found that in order to view the microspheres clearly, the exposure time had to be increased to 1500 μs. This may have been because the microspheres contain a shell that is relatively thick compared to the lines on the resolution target, requiring stronger illumination in order to be viewed. Under these conditions, the 0.5-μm-diameter microspheres were resolvable. This was further confirmed by the fact that two of the spheres, which were located side by side, could be easily distinguished from one another.

It was determined that, according to the pixel-to-micron conversion scale (7.9 pixels/μm), the diameter of each microsphere appeared to be much larger than 0.5 μm. This was a result of Fresnel diffraction, which produces a circular diffraction pattern, making the objects appear much larger than they actually are. Therefore, it was determined that the exact location of the microsphere was somewhere within the center of the diffraction pattern. Figure 12 shows images of the microspheres, which were captured by the digital microscope and then analyzed using Matlab software to determine the actual location of the microsphere. Image (a) shows the original image of the microspheres. The black square within the image indicates the portion of the image that was extracted to produce image (b). Image (b) shows a light intensity map of the microspheres, in which a color gradient is used to show differences in light intensity across the image. The areas with lower light intensity indicated the presence of an object. The black square within image (b) indicates the single microsphere that was extracted to produce image (c). Image (c) shows a re-scaled light intensity map of the single microsphere and the diffraction

surrounding it. The white square indicates the exact location of the microsphere.
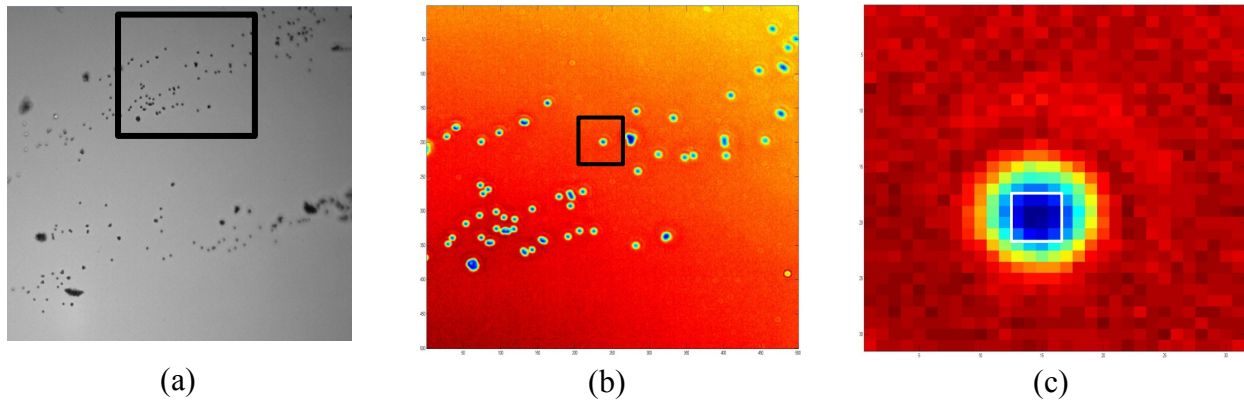

<center>(a)   (b)   (c)</center>

Figure 12. Images of microspheres taken by the digital microscope and analyzed using Matlab. Image (a) shows the original image, taken with the blue LED and a 40x objective. Image (b) shows a light intensity map of a portion of the original picture. Image (c) shows a re-scaled light intensity map of a single microsphere from the original image (from Ref. 7).

The ability of the digital microscope to resolve defects upon the surface of a CH cryo shell was then tested using the same Matlab analysis method. Figure 13 shows images of the CH cryo shell that were taken with a blue LED, a 40x objective, a current of 1400 mA, and an exposure time of 800 μs. Image (a) shows the original image of the CH cryo shell, containing several defects upon its surface. The black square within the image indicates the portion of the image that was extracted to produce image (b). Image (b) shows a light intensity map of the defects. The black square within image (b) indicates the single defect that was extracted to produce image (c). Image (c) shows a re-scaled light intensity map of the single defect and the diffraction surrounding it. Upon analyzing these defects, it was found that, like the 0.5 μm diameter microsphere, one particular defect contained a 4×4 pixel region within its center (shown by the white square). Therefore, according to the pixel-to-micron conversion scale, it was determined that this defect had an approximate diameter of 0.5 μm, demonstrating that, under optimized conditions, the digital microscope was able to resolve 0.5 μm diameter defects, within a room temperature setting.
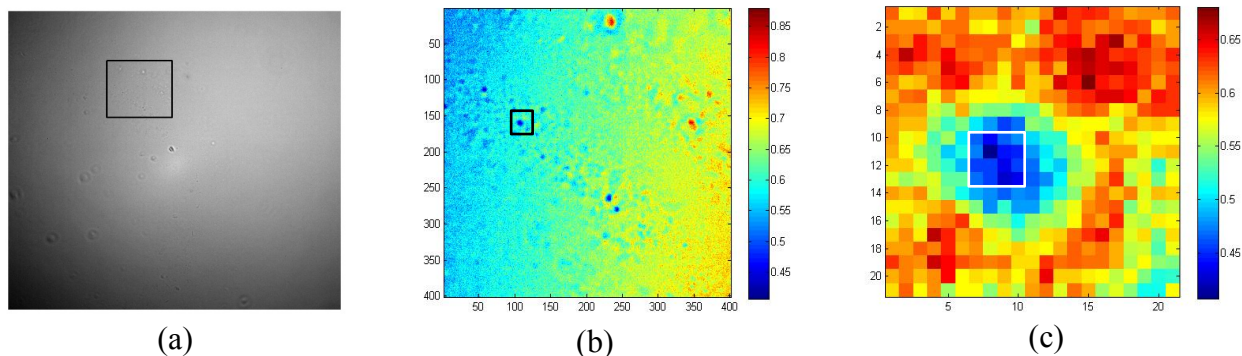
(a) (b) (c)

Figure 13. Images of defects upon the CH cryo shell taken by the digital microscope and analyzed using Matlab. Image (a) shows the original image, taken with a blue LED and a 40x objective. Image (b) shows a light intensity map of a portion of the original picture. Image (c) shows a re-scaled intensity map of a single defect from the original image (from Ref. 7).

6. Discussion

The digital microscope was able to demonstrate a resolving power of 0.5 μm with polymer microspheres and defects on the surface of a CH cryo shell. Additionally, it was determined that the optimal working conditions for the digital microscope utilized a 40x objective and a blue LED, with a current of 1400 mA, and an exposure time of 800 μs. These conditions produce the optimal resolving power ($\sim$0.5 μm) for the digital microscope in a room temperature environment for a US Air Force Resolution Target.

However, it should be noted that different working conditions might be required for certain operations. For example, in order to view polymer microspheres, the LED's exposure time needed to be increased. Additionally, the working conditions may need to be adjusted in order to view CH cryo shells that are filled with DT fuel. The digital camera may also respond to the cryogenic environment and vacuum pressure within the cryostat differently than it does to the room temperature environment in which it was optimized. Its working conditions may need to be

adjusted according to the nature of the defects that it is viewing. Additionally, although the 40x objective was determined to provide the optimal magnification in order to view submicron defects, it also contains a much smaller depth of field than objectives with lower magnification. Therefore, the camera is only able to focus on a small portion of the target surface. Future work may be required to overcome these limitations and allow the camera to focus on larger portions of the target. Furthermore, because simply viewing target defects from the side has proven to be difficult due to the curvature of the target, a more efficient method for measuring the height or depth of target defects may need to be developed.

7. Acknowledgements

8. References

[1] R.S. Craxton et al., "Direct-Drive Inertial Confinement Fusion: A Review." *Physics of Plasmas* 22, 110501 (2015).

[2] T.C Sangster et al., "Cryogenic DT and D_2 Targets for Inertial Confinement Fusion." *Physics of Plasmas* 14, 058101 (2007).

[3] "Chapter 1: CTHS Overview," *Cryogenic Target Handling System Operations Manual, Volume IV – CTHS Description* (LLE) 1, 3 (2004)

[4] R. Janezic, private communication

[5] R. Janezic et al., (2016, June). "Planning meeting for High School Summer Student Project involving an FTS #2 Digital Microscope for Defect Evaluation," presentation at High School Summer Student Preparation Meeting.

[6] Thermo Fisher Scientific, Waltham, Massachusetts, 02451

[7] D. Comfort, private communication